Induced Coiling Action: Exploring the Intrinsic Defects in Five-Fold Twinned Silver Nanowires

Liangfang Zhu,[†] Xiaoshuang Shen,[†] Zhiyuan Zeng,[‡] Hong Wang,[†] Hua Zhang,[‡] and Hongyu Chen[†,*]

[†]Division of Chemistry and Biological Chemistry, Nanyang Technological University, Singapore 637371, and [‡]School of Materials Science and Engineering, Nanyang Technological University, Singapore 639798

ABSTRACT

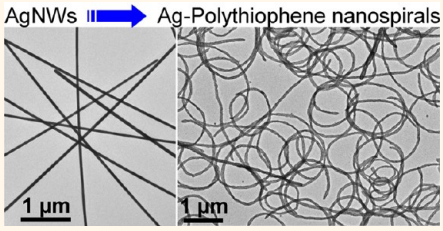

Growth of polythiophene (PTh) on five-fold twinned Ag nanowires (NWs) is not symmetrical due to preferred etching of their intrinsic defects. This imbalance of polymer formation leads to consistent bending action along the etched NWs, coiling the resulting Ag-PTh nanocomposites into planar spirals. We studied the etching intermediates and also the effects of the surface ligands in order to understand the symmetry-breaking action. The defect-dependent etching chemistry offers a new means to induce motion and a novel perspective in the ordered occurrence of certain defects. We demonstrate that Ag can be deposited back onto the coiled Ag-PTh composite to form metallic spirals.

KEYWORDS: induced coiling · silver nanowires · defects · selective etching · polythiophene

Many devices in our daily life achieve their functions by mechanical motion. However, doing so at the nanoscale involves great challenges. Indeed, the motions of known nanostructures are, in most cases, passive as they were induced by either random Brownian forces or direct manipulation. Active motions are rare and mostly achieved by large structures. Several types of micrometer-sized swimmers were known, whereby anisotropic reaction rates on their surface led to translational propulsion.[1−5] Their large size is of critical importance because it evens out the effects of Brownian force, so that external electric or magnetic field could exert influence on the colloidal architectures to achieve effective movement.[5] At the nanoscale, however, Brownian motion disrupts any translational movement. Thus, conformational motions are of greater importance because they are less affected. The shape transformation of biomolecules, for example, can reliably occur despite strong Brownian forces. Actually, the stimuli-responsive conformational changes of proteins, such as ATP synthase and myosin, provide the basis for enzymatic activity and cell motility.

In comparison, man-made nanostructures have yet to advance in complexity in order to achieve simple predictable (*i.e.*, not random) motion. Previously, we have shown that contracting polymer shells can exert force to embedded nanofilaments such as Au nanowires (NWs) and carbon nanotubes, forcing them into ring structures.[6,7] Moreover, Au−Ag alloy NWs with twisted lattice were transformed to double helices upon growth of an additional metal layer.[8] While these systems have yet to achieve motions of practical significance, they are the initial steps toward motility in future nanodevices. The key challenge is to broaden the scope of active nanostructures, identifying and understanding processes that can drive consistent motion.

NWs are basic building blocks in nanotechnology.[9−13] Relatively speaking, it is easier to generate orderly conformational changes in one-dimensional (1D) wires than in 2D sheets. Understanding the structural characteristics of various types of NWs is critical for exploring new ways of creating motion. For five-fold twinned AgNWs, it is known that the five-fold symmetry is incompatible with the face-centered cubic (fcc) packing of Ag lattice, leaving a misfit angle of 7.35° in their cross section (Figure 1a).[14−16] When their diameter is below 100 nm, the defects caused by this theoretical "gap" are hardly detectable,[17] and thus, their side facets appeared to be symmetrically equivalent.

* Address correspondence to hongyuchen@ntu.edu.sg.

Received for review March 13, 2012 and accepted June 19, 2012.

Published online June 19, 2012
10.1021/nn301096n

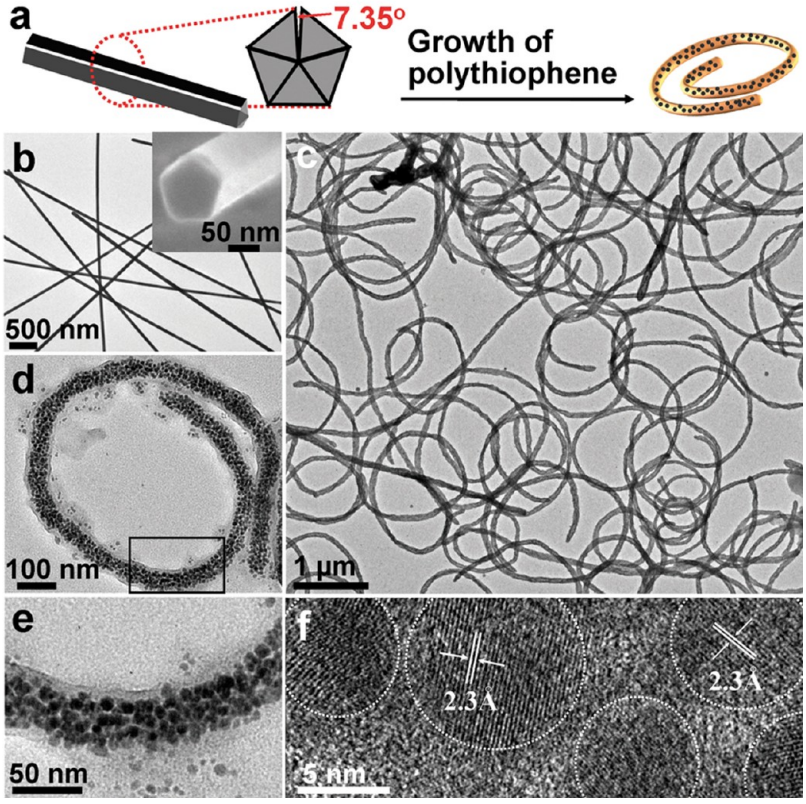

Figure 1. (a) Schematics illustrating the theoretical "gap" in the cross section of pentagonal AgNWs; TEM images of (b) AgNWs (inset: SEM image of an end); (c,d) unidirectionally coiled Ag-PTh spirals; (e) magnified view of the bracketed region in d; and (f) HRTEM image of the embedded AgNPs (see the Supporting Information for EDS analyses; the AgNPs are denoted by circles).

In this paper, we show that the defects resulting from the angular misfit probably occur on the *same* side of AgNWs. We coat polythiophene (PTh) on AgNWs, which are partially etched during the process. Intriguingly, the preferred etching of defects in AgNWs breaks their five-fold symmetry and causes unidirectional bending action. After etching, the remaining Ag nanoparticles (NPs) are embedded in PTh, forming nanocomposites that appear as planar spirals (Figure 1). We focus our study on the source of the coiling action, which offers not only a new means to induce motion but also an alternative evidence for the ordered defects in pentagonal AgNWs.

RESULTS AND DISCUSSION

We synthesized AgNWs (d = 70−100 nm; l = 3−10 μm) by polyol reduction method using polyvinylpyrrolidone (PVP) as the capping agent.[18] After repeated centrifugation and washing with ethanol to remove excess PVP, the purified AgNWs were stored in ethanol and characterized by transmission electron microscopy (TEM, Figure 1b). They were straight with a smooth surface. As judged from their ends (inset of Figure 1b), they have pentagonal cross section, consistent with those reported in the literature.[19,20]

We used the Fenton's reagent,[21] a combination of $FeCl_2$ and H_2O_2, to oxidize thiophene in the presence of AgNWs and sodium dodecylsulfate (SDS). Briefly, SDS (final concentration of 6.7 mM, same below), thiophene (96 mM), catalytic amount of $FeCl_2$ (17 μM), H_2O_2 (62 mM), and HCl (1.3 mM) were mixed thoroughly in a glass vial.[22] Then, AgNWs (1.45 mM in Ag atoms) were added; the mixture was vortexed for 10 s before it was heated at 75 °C for 2 h. The color of the solution quickly (within 2 min) turned from the gray color of AgNWs to dark brown, indicating polymerization of thiophene to PTh.[23,24] After cooling to room temperature, the mixture was diluted with water. The product was isolated by centrifugation before TEM characterization.

To our great interest, the originally straight AgNWs were transformed to spirals (Figure 1c). The Ag-PTh nanocomposite must have bent along a *same* direction in order to create the near-circular shape. Among the 220 spirals surveyed, 94% of them have unidirectional curvature (the remaining 6% were either nearly straight or have random curvature).[22] Close inspection of the spirals revealed that the AgNWs have been etched into discrete NPs (d = 10 ± 2 nm, Figure 1d,e). Figure 1f shows their high-resolution TEM (HRTEM) image; the well-resolved and continuous fringes were characteristic of Ag nanocrystals. These separated AgNPs were embedded in and bound together by the polymer shell, retaining the rough form of wires. However, the diameter of these cylindrical clusters was

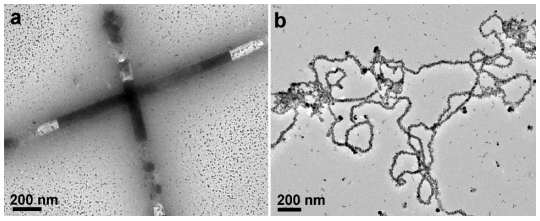

Figure 2. Control experiments showing that (a) at neutral pH, AgNWs were not completely etched even after 10 h. The etched section was completely removed but did not bend; and (b) when the concentration of thiophene was reduced, randomly coiled Ag-PTh nanocomposites were obtained.

only 45 ± 10 nm, significantly smaller than that of the original AgNWs (70−100 nm). Thus, the nanocomposites must have collapsed inward after the etching and polymerization. Energy-dispersive X-ray spectroscopy (EDS) analyses confirmed the presence of Ag and S in the core−shell structure,[22] supporting Ag-PTh composition therein.

Obviously, there were two parallel processes leading to the formation of Ag-PTh spiral: etching of AgNW and polymerization of thiophene. The Fenton's reagent produces radical species ($HO^{\bullet}$ and $HOO^{\bullet}$)[21] that can act as oxidants for both reactions. Previously, we reported the *in situ* polymerization of thiophene to PTh on the surface of AuNPs in a pH neutral SDS solution.[24] It was found that the surfactant SDS adsorbed on the hydrophobic thiophene-functionalized AuNPs, facilitating thiophene oxidation at the aqueous interface.[25−28] In comparison, in the current system, the AgNWs were more prone to oxidation than AuNPs. Moreover, acidic medium (pH 4) was used to improve the rate of formation and stability of the oxidative radicals.[29] The reason that Ag was not completely etched was likely because the PTh shell protected the remaining AgNPs against further reactions (*vide infra*). Control experiments carried out at neutral pH went much slower: even after reacting for 10−24 h, the AgNWs were still not completely etched (Figure 2a). The PTh in the etched sections did not bend, and Ag was almost completely removed from these parts.

We were intrigued by the shape transformation of straight NWs to spirals and thus focused our study on the source of the *symmetry-breaking* action. While it is hard to imagine how polymer can be deposited in defiance of the NW's five-fold symmetry, the PTh shell is the only means to achieve concerted action among the discrete AgNPs. In other words, the PTh shell likely played an *indirect* role following an initial symmetry-breaking process, offering an important clue.

When both thiophene and H_2O_2 were increased in concentration, the resulting PTh shell became thicker without noticeable change in terms of spiral formation.[22] When less thiophene (32 mM) was used, the obtained nanocomposites were randomly coiled (Figure 2b). This clear contrast between ordered and

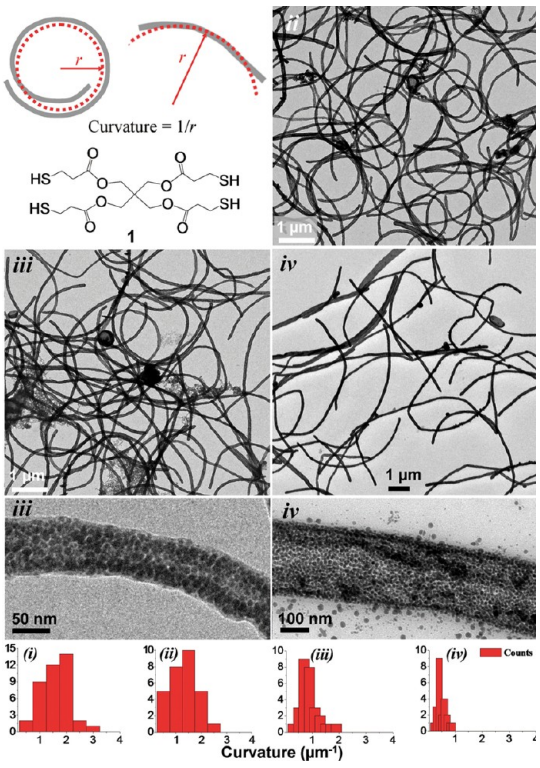

Figure 3. Schematics showing the definition of curvature and compound 1 and TEM images of the Ag-PTh nanocomposites synthesized from 1-modified AgNWs, where (*i*) 0 μM (the same sample as shown in Figure 1c), (*ii*) 9.6 μM, (*iii*) 16 μM, and (*iv*) 22.4 μM of 1 was used. The planar spirals are fitted to circles of roughly same radii. The curvature (μm^{-1}) is calculated as the reciprocal of radius. The bottom panel shows the respective histograms of the curvature distributions.

disordered coiling ruled out external factors such as centrifugation or drying as the cause. The coiling was likely induced by imbalanced strain/pressure in the nanocomposite during its inward collapsing, and thus, the amount of PTh buildup depended critically on the initial thiophene concentration. However, this buildup has to somehow break the five-fold symmetry, likely a consequence of preferential etching in the AgNWs.

We tried to modify the surface ligands on the AgNWs to modulate their etching. The as-synthesized AgNWs were covered with PVP, which was known to have specific affinity for Ag(100) facets.[30] It is likely that the surface-adsorbed PVP has not been fully removed after purification. This specific affinity may lead to preferred etching of unprotected facets or defects. To test this hypothesis, we treated the purified AgNWs with a small amount of stronger ligand, $C(CH_2OCOCH_2CH_2SH)_4$ (denoted as **1**, Figure 3) before PTh was grown. This ligand was supposed to adsorb on the Ag facets nonspecifically and, thus, reduce the unevenness in terms of Ag etching. It was found that the **1**-modified AgNWs underwent similar unidirectional bending but to a lesser extent. To compare these results, we fit the

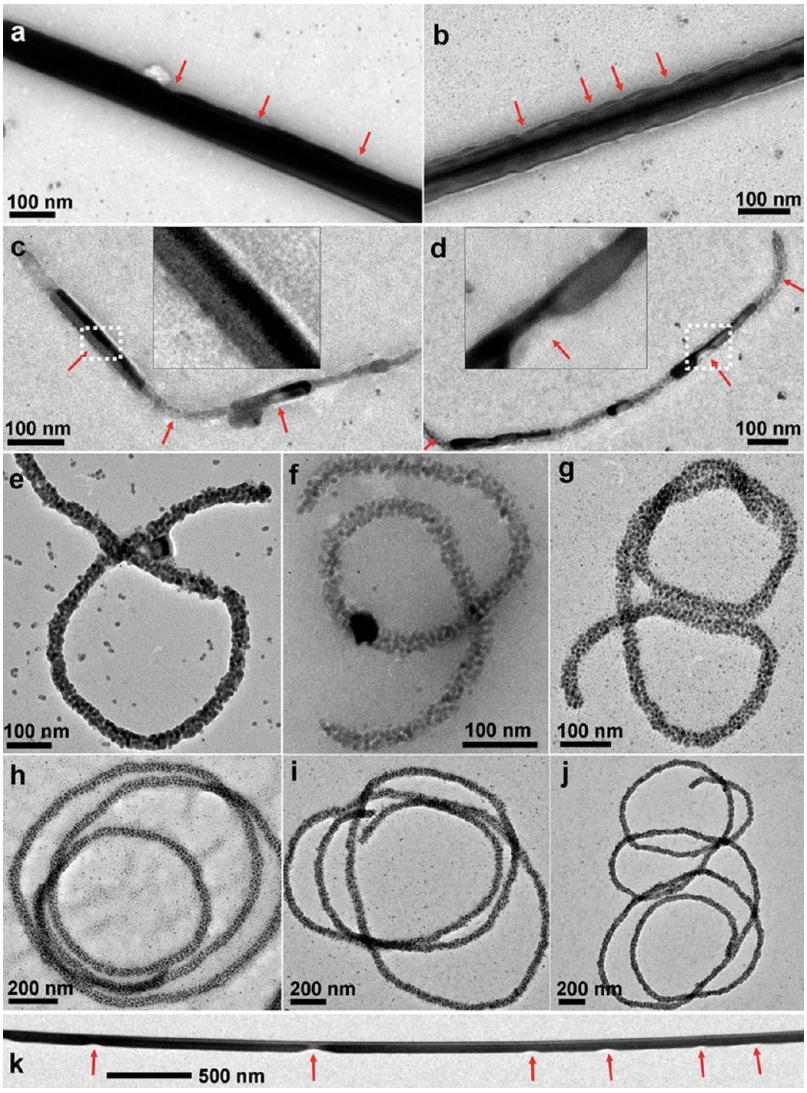

Figure 4. TEM images of Ag-PTh intermediates isolated at (a) 1 min, (b) 3 min, (c,d) 4 min, and (e−g) 6 min after the reaction started (T = 50 °C); (h−j) Ag-PTh spirals obtained using long AgNWs; (k) AgNWs etched by incubating with 1 only. The arrows indicate the side that was preferentially etched.

planar spirals to circles of roughly the same radius and obtain their curvature (μm^{-1}) as reciprocal of radius. With 9.6 μM of **1** treating the AgNWs, the curvature of the resulting nanocomposites (Figure 3*ii*) was noticeably smaller than those without the treatment (Figure 1c). When the concentration of **1** was increased to 16 and 22.4 μM (Figure 3, *iii* and *iv*), the curvatures of the obtained spirals were further reduced, indicating a strong correlation between the surface density of **1** and the extent of NW bending. Most likely, replacing PVP with **1** reduced the difference in reactivity for the Ag facets and, thus, reduced the effects of symmetry-breaking in terms of Ag etching.

With the increase of concentration of **1**, the resulting Ag-PTh nanocomposites also became increasingly tube-like (Figure 3, *iii* and *iv*).[22] Their completely etched interior indicated that the presence of PTh was essential for retaining the residue AgNPs. It appeared that the presence of **1** had dramatically slowed the thiophene diffusion into the etched NWs. As a result, only the surface layer of Ag was protected by PTh, causing the inner Ag domain to be completely etched, in a way similar to Ag structures that were oxidized by $HAuCl_4$.[31,32]

To study the early stage of Ag etching and PTh formation, we reduced the reaction temperature from 75 to 50 °C; all other conditions were unchanged from those of Figure 1c. With reactions slowed, aliquots of the solution were isolated at different time points (t = 1−6 min) and the products were characterized. At t = 1 min, small pits appeared on one side of AgNWs (Figure 4a). At t = 3 min, pits appeared on both sides, but the ones on one side were deeper than those on the other (Figure 4b). Scanning electron microscopy (SEM) characterization of the etched products did not reveal additional information owing to limited resolution and interference from organic/polymer deposit.

At $t = 4$ min, serious etching set in and only a few half-etched segments of AgNWs still remained (Figure 4c,d). It should be noted here that small AgNPs (such as those in Figure 1f) did appear inside the etched sections, but because of the large difference in TEM contrast against the unetched Ag blocks, they were hardly visible. Bending of nanocomposites can now be observed; the direction was such that the preferentially etched side was always on the outside of the curve. This can be explained by the imbalanced formation of PTh inside the etched AgNWs: the PTh buildup likely caused internal pressure in the nanocomposite, which should be more pronounced on the side that was etched first.

At $t = 6$ min, most of the original AgNWs were etched away (Figure 4e−g). Nearly all of the nanocomposites were bent unidirectionally, forming 1−2 loops. At this stage, there was no overcoating PTh layer, and thus, PTh must have formed *inside* the nanocomposites holding the remaining AgNPs together. When longer AgNWs (8−10 μm) were used, spirals with multiple loops can be obtained (Figure 4h−j). The difference in the curvature of the loops was small relative to the large difference among the individual NWs in Figure 3. It could be caused by the variation in the defects along the original AgNWs or by the drying process. It is expected that the collapsing of 3D conformation onto the 2D substrate or the flow of residue solvent could affect the final curvatures that we observed.

The preferential etching of defects should be general to other etching methods. Thus, we sought an alternative method to obtain clearer etching results without the influence of polymer. A solution of ligand **1** (0.5 mM) was used to slowly etch purified AgNWs over a prolonged period (17 h). The resulting AgNWs showed clear signs of corrosion, and most notably, the initial corrosion *always* occurred on the same side (Figure 4k; see additional examples in the Supporting Information). The consistent formation of these pits, as opposed to their random occurrence, breaks the symmetry of the pentagonal AgNWs and, thus, can be correlated to the subsequent unidirectional action.

On the basis of this result, we postulate that the preferential etching probably started at the angular-misfit defects. While such misfit is known, only in micrometer-sized decahedra and thick Ag rods ($d >$ 700 nm) did the resulting defects become directly observable by electron microscopy.[17] They appeared as re-entrant grooves along one of their side facets. In thin AgNWs ($d <$ 100 nm), however, there was no obvious anomaly and the defects were only observable by cross-sectional TEM.[33,34] Typically, the defects located at two or three of the five twinning boundaries. In all known accounts, the angular-misfit defects are block defects, whereas the twinning defects are mostly restricted in a plane of a few atoms in thickness. Obviously, etching of the five twinning defects in the AgNWs cannot explain the symmetry-breaking action.

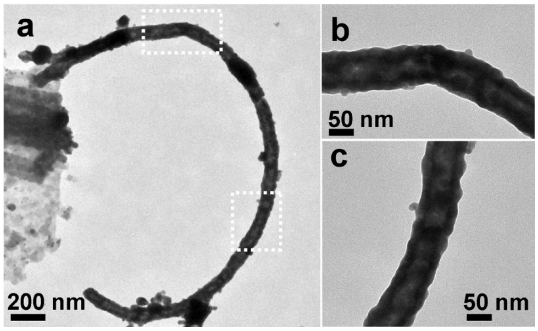

Figure 5. TEM images of (a) Ag nanospiral after depositing Ag on Ag-PTh nanocomposite, and (b,c) its magnified sections.

On the other hand, the angular-misfit defects could occur on only one side of AgNWs. They are also larger in size and should be more easily etched.

It should be noted that the physical characterization methods such as cross-sectional TEM are effective for analyzing a few sections of individual NWs, but it is extremely difficult to obtain information on the spatial distribution of defects and, particularly, the extent of occurrence among the different individuals in a sample.

Putting this together, the Ag-PTh spiral formation can be explained as follows. The Ag(100) facets are protected by PVP, but less so for the angular-misfit defects. Thus, when AgNWs are mixed with Fenton's reagent, the oxidative radicals preferentially react with the defective regions, causing the initial pits to occur there. This initial advantage is magnified by the fast subsequent reactions (finished within 4 min even at 50 °C). The freshly exposed Ag surface in the pits and the faster rate of diffusion at the nearby cavities probably promote the etching and polymerization reactions. The formation of PTh inside the AgNWs is supported by Figure 4e−g, and there is good reason to believe that the amount of infiltrated PTh is inhomogeneous due to favorable reactions at the defective sites. Excess PTh buildup at such sites probably leads to imbalanced internal pressure that bends the nanocomposite during its inward collapse (leading to smaller diameter). Missing some materials in the initial pits should not preset the bending direction because it is equivalent to bending a thinner wire. It would not be easier to bend the pitted AgNWs toward any particular direction.

When the amount of thiophene used in the reaction is reduced (Figure 2b), the less amount of PTh formation leads to less internal pressure, resulting in random coiling. This proposal explains the observation that the preferentially etched side with more polymer is always on the outside of the curve (Figure 4c,d). The fact that most of the nanocomposites were unidirectionally coiled suggests that the angular-misfit defects probably occur on the same side of AgNWs. Such single-sided preferential etching is supported by the etching intermediates (Figure 4a,b,k). When AgNWs are

pretreated with **1**, the stronger ligand replaces the surface PVP and binds nonspecifically, reducing the effects of symmetry breaking in terms of Ag etching. Moreover, this ligand layer also reduces the amount of infiltrated PTh and thus the extent of bending (Figure 3). In sample 3*iii* and 3*iv*, the central portion of AgNWs is completely etched because of the lack of PTh formation there. This argument is consistent with the protection of the AgNPs embedded in PTh domains. When the reaction is carried out at neutral pH (Figure 2a) or with reduced reactants (Figure 2b), bending was not achieved, highlighting the importance of fast reactions.

As a proof-of-concept demonstration, we deposited Ag back into the Ag-PTh nanocomposites, aiming to develop a method for fabricating metal nanospirals or even split rings.[35,36] We used the sample that is shown in Figure 3*iii*, so that the AgNPs were more exposed to the solvent because of the thinner PTh shell. These nanocomposites were treated with 23.5 mM $AgNO_3$ at 50 °C for 2 h. After centrifugation to remove the excess $AgNO_3$, the product was redispersed in 34 mM sodium citrate in DMF, and the mixture was incubated at 90 °C for 2 h to reduce the adsorbed Ag^+ ions. Here, DMF was used to slow down the reduction reaction,[8] in order to favor uniform deposition of Ag. Finally, the product was isolated by centrifugation and characterized. As shown in Figure 5, the deposited Ag formed a continuous layer connecting the AgNPs in PTh. Most importantly, the curved "C" shape was retained in the metallic nanostructure.

CONCLUSIONS

The unidirectional coiling action of AgNWs was a result of synergistic effects of preferred etching and PTh growth. The defect-specific etching chemistry provides alternative evidence for the spatial distribution of defects in pentagonal AgNWs. In contrast to the traditional physical characterization methods, the etching chemistry of AgNWs reveals their properties through the induced coiling action of a large number of NWs. On the basis of the obtained nanospirals, we conclude that the angular-misfit defects probably occur on the *same* side of AgNWs for several micrometers in length.

Most importantly, the coiling behavior of the nanocomposites is a conformational change induced by chemical stimuli, not by direct manipulation. It provides a new means to create motion at the nanoscale, which could be potentially exploited as actuators in the future development of smart nanodevices. Consistently curved nanowires are extremely rare. The redeposition of Ag on curved nanowires is a first step in advancing this new synthetic methodology.

MATERIALS AND METHODS

Materials. All chemical reagents were used as purchased without further purification. Polyvinylpyrrolidone (PVP-K30, M_W = 40 000), silver nitrate ($AgNO_3$, 99%), and pentaerythritol tetrakis(3-mercaptopropionate) ($C(CH_2OCOCH_2CH_2SH)_4$, referred to as **1**) were purchased from Aldrich. Thiophene (99%), aniline (99%), sodium dodecylsulfate (SDS, 99%), ferrous chloride tetrahydrate ($FeCl_2 \cdot 4H_2O$, 99%), and hydrogen peroxide (H_2O_2, 30% w/w) were purchased from Alfa Aesar. Ethylene glycol (EG) was purchased from J.T. Baker. Copper specimen grids (300 meshes) with carbon film (TEM grids) were purchased from Beijing XXBR Technology Co. Deionized (DI) water (resistance >18.2 $M \cdot cm^{-1}$) was used in all of our experiments.

Characterization. TEM images were collected on a JEM-1400 (JEOL) transmission electron microscope operated at 100 kV. High-resolution TEM images and energy-dispersive X-ray spectroscopy (EDS) analyses were taken from JEM 2100F (JEOL) transmission electron microscope operated at 200 kV. SEM images were collected from a JEOL-6700F scanning electron microscope operated at 10 kV.

Preparation of TEM Samples. TEM grids were treated with oxygen plasma in a Harrick plasma cleaner/sterilizer for 1 min to improve the surface hydrophilicity. The grid was placed face-down on a droplet of as-synthesized sample laid on a plastic Petri dish. A filter paper was used to wick off the excess solution on the TEM grid, which was then dried in air for 10 min.

Synthesis of AgNWs. The AgNWs (d = 70−100 nm; l = 3−10 μm) were synthesized by polyol reduction method using PVP as the capping agent.[18] Typically, 5 mL of EG containing 40 mg/mL of PVP was intensively stirred at 160 °C for 1 h. Then, a solution of 0.12 M of $AgNO_3$ in 3 mL of EG was injected into the mixture at a rate of 0.125 mL/min. The reaction was continuously stirred for another 1 h. The color of the mixture turned from light-yellow to yellow, orange, orange-red, green, gray-brown, and finally gray-green. After cooling to room temperature, the mixture was centrifuged (200*g*/20 min) and washed with ethanol for a total of three cycles to remove the excess PVP and EG. The purified AgNWs were stored in ethanol for use (22.5 mM in Ag atoms).

Synthesis of Ag-PTh Nanospirals. The purified AgNWs (100 μL) were concentrated to a total volume of 10 μL by centrifugation at 200*g* for 20 min. After removal of supernatant, the isolated AgNWs were added to a mixture that contained SDS (7 mM, 1.5 mL), thiophene (12−20 μL), $FeCl_2$ (1 mM, 26 μL), H_2O_2 (10−20 μL), and HCl (0.1 mM, 20 μL). The final solution had a total volume of 1.568 mL, where [Ag atom] = 1.45 mM, [thiophene] = 96−160 mM, [SDS] = 6.7 mM, [$FeCl_2$] = 16.6 mM, [H_2O_2] = 62−124 mM, and [HCl] = 1.3 mM. The mixture was vortexed for 10 s before being heated at 75 °C for 2 h. After cooling to room temperature, the mixture was diluted with water. The product was isolated by centrifugation at 2000*g* for 20 min.

To monitor the structural transformation from straight AgNWs to the Ag-PTh nanospirals, a control experiment was carried out at 50 °C while keeping all other conditions unchanged. With slower reaction at the lower temperature, 200 μL aliquots of the reaction mixture were extracted at different time points (1−6 min); they were immediately diluted with water. The products were isolated by centrifugation at 2000*g* for 20 min before TEM characterization.

Modification of AgNWs by Ligand 1. One hundred microliters of purified AgNWs was concentrated to a total volume of 10 μL by centrifugation at 200*g* for 20 min. Then, 3−7 μL of **1** (5 mM, in ethanol) was added, corresponding to Figure 3, *ii*−*iv*. The mixture (about 13−17 μL) was thoroughly mixed and incubated at room temperature for 30 min before use.

Etching of AgNWs by Ligand 1. Ten microliters of **1** (5 mM, in ethanol) was mixed with 100 μL of purified AgNWs. The mixture was incubated in open air at room temperature for 17 h with

continuous shaking. The product was isolated by centrifugation at 200*g* for 20 min before TEM characterization (Figure 4k).

Regrowth of Ag on Ag-PTh Nanospiral. The Ag-PTh nanospiral was immersed in $AgNO_3$ solution (23.5 mM, 200 μL) at 50 °C for 2 h. After centrifugation to remove the excess $AgNO_3$, sodium citrate (34 mM, 200 μL) and DMF (50 μL) were added. The mixture was incubated at 90 °C for 2 h to allow the slow growth of Ag. The product was purified by centrifugation at 2000*g* for 15 min.

Conflict of Interest: The authors declare no competing financial interest.

Acknowledgment. The authors thank the MOE (ARC 13/09) and A*Star (102-152-0018) of Singapore for the financial support.

Supporting Information Available: Details for experimental procedures, EDS results, and large-area views of TEM images. This material is available free of charge *via* the Internet at http://pubs.acs.org.

REFERENCES AND NOTES

1. Wang, J. Can Man-Made Nanomachines Compete with Nature Biomotors? *ACS Nano* **2009**, *3*, 4–9.
2. Ebbens, S. J.; Howse, J. R. In Pursuit of Propulsion at the Nanoscale. *Soft Matter* **2010**, *6*, 726–738.
3. Mirkovic, T.; Zacharia, N. S.; Scholes, G. D.; Ozin, G. A. Nanolocomotion—Catalytic Nanomotors and Nanorotors. *Small* **2010**, *6*, 159–167.
4. Thakur, S.; Chen, J. X.; Kapral, R. Interaction of a Chemically Propelled Nanomotor with a Chemical Wave. *Angew. Chem., Int. Ed.* **2011**, *50*, 10165–10169.
5. Wang, J.; Manesh, K. M. Motion Control at the Nanoscale. *Small* **2010**, *6*, 338–345.
6. Xu, J.; Wang, H.; Liu, C. C.; Yang, Y. M.; Chen, T.; Wang, Y. W.; Wang, F.; Liu, X. G.; Xing, B. G.; Chen, H. Y. Mechanical Nanosprings: Induced Coiling and Uncoiling of Ultrathin Au Nanowires. *J. Am. Chem. Soc.* **2010**, *132*, 11920–11922.
7. Chen, L. Y.; Wang, H.; Xu, J.; Shen, X. S.; Yao, L.; Zhu, L. F.; Zeng, Z. Y.; Zhang, H.; Chen, H. Y. Controlling Reversible Elastic Deformation of Carbon Nanotube Rings. *J. Am. Chem. Soc.* **2011**, *133*, 9654–9657.
8. Wang, Y.; Wang, Q. X.; Sun, H.; Zhang, W. Q.; Chen, G.; Wang, Y. W.; Shen, X. S.; Han, Y.; Lu, X. M.; Chen, H. Y. Chiral Transformation: From Single Nanowire to Double Helix. *J. Am. Chem. Soc.* **2011**, *133*, 20060–20063.
9. Sun, Y. G. Silver Nanowires—Unique Templates for Functional Nanostructures. *Nanoscale* **2010**, *2*, 1626–1642.
10. Ma, D. D. D.; Lee, C. S.; Au, F. C. K.; Tong, S. Y.; Lee, S. T. Small-Diameter Silicon Nanowire Surfaces. *Science* **2003**, *299*, 1874–1877.
11. Zhang, Y. W.; Yan, Z. G.; You, L. P.; Si, R.; Yan, C. H. General Synthesis and Characterization of Monocrystalline Lanthanide Orthophosphate Nanowires. *Eur. J. Inorg. Chem.* **2003**, 4099–4104.
12. Huang, X. Q.; Zheng, N. F. One-Pot, High-Yield Synthesis of 5-Fold Twinned Pd Nanowires and Nanorods. *J. Am. Chem. Soc.* **2009**, *131*, 4602–4603.
13. Sun, Z. H.; Ni, W. H.; Yang, Z.; Kou, X. S.; Li, L.; Wang, J. F. pH-Controlled Reversible Assembly and Disassembly of Gold Nanorods. *Small* **2008**, *4*, 1287–1292.
14. Martin, T. P. Shells of Atoms. *Phys. Rep.* **1996**, *273*, 199–241.
15. Marks, L. D. Experimental Studies of Small-Particle Strutures. *Rep. Prog. Phys.* **1994**, *57*, 603–649.
16. Xia, Y. N.; Xiong, Y. J.; Lim, B.; Skrabalak, S. E. Shape-Controlled Synthesis of Metal Nanocrystals: Simple Chemistry Meets Complex Physics? *Angew. Chem., Int. Ed.* **2009**, *48*, 60–103.
17. Zhang, W. J.; Liu, Y.; Cao, R. G.; Li, Z. H.; Zhang, Y. H.; Tang, Y.; Fan, K. N. Synergy between Crystal Strain and Surface Energy in Morphological Evolution of Five-Fold-Twinned Silver Crystals. *J. Am. Chem. Soc.* **2008**, *130*, 15581–15588.
18. Sun, Y. G.; Xia, Y. N. Large-Scale Synthesis of Uniform Silver Nanowires through a Soft, Self-Seeding, Polyol Process. *Adv. Mater.* **2002**, *14*, 833–837.
19. Gao, Y.; Jiang, P.; Liu, D. F.; Yuan, H. J.; Yan, X. Q.; Zhou, Z. P.; Wang, J. X.; Song, L.; Liu, L. F.; Zhou, W. Y.; *et al.* Synthesis, Characterization and Self-Assembly of Silver Nanowires. *Chem. Phys. Lett.* **2003**, *380*, 146–149.
20. Xia, Y. N.; Yang, P. D.; Sun, Y. G.; Wu, Y. Y.; Mayers, B.; Gates, B.; Yin, Y. D.; Kim, F.; Yan, Y. Q. One-Dimensional Nanostructures: Synthesis, Characterization, and Applications. *Adv. Mater.* **2003**, *15*, 353–389.
21. Chen, G. Z. A Golden Episode Continues Fenton's Colorful Story. *Angew. Chem., Int. Ed.* **2010**, *49*, 5413–5415.
22. See the Supporting Information for details.
23. Lee, S. J.; Lee, J. M.; Cheong, I. W.; Lee, H.; Kim, J. H. A Facile Route of Polythiophene Nanoparticles *via* Fe^{3+}-Catalyzed Oxidative Polymerization in Aqueous Medium. *J. Polym. Sci., Part A: Polym. Chem.* **2008**, *46*, 2097–2107.
24. Sun, H.; He, J. T.; Xing, S. X.; Zhu, L. F.; Wong, Y. J.; Wang, Y. W.; Zhai, H. J.; Chen, H. Y. One-Step Synthesis of Composite Vesicles: Direct Polymerization and *In Situ* Over-Oxidation of Thiophene. *Chem. Sci.* **2011**, *2*, 2109–2114.
25. Sindoro, M.; Feng, Y. H.; Xing, S. X.; Li, H.; Xu, J.; Hu, H. L.; Liu, C. C.; Wang, Y. W.; Zhang, H.; Shen, Z. X.; Chen, H. Y. Triple-Layer (Au@Perylene)@Polyaniline Nanocomposite: Unconventional Growth of Faceted Organic Nanocrystals on Polycrystalline Au. *Angew. Chem., Int. Ed.* **2011**, *50*, 9898–9902.
26. Xing, S. X.; He, J. T.; Liu, X. C.; Chen, H. Y. A Symmetry-Adapted Shell Transformation of Core−Shell Nanoparticles for Binary Nanoassembly. *Chem. Commun.* **2011**, *47*, 12533–12535.
27. Xing, S. X.; Feng, Y. H.; Tay, Y. Y.; Chen, T.; Xu, J.; Pan, M.; He, J. T.; Hng, H. H.; Yan, Q. Y.; Chen, H. Y. Reducing the Symmetry of Bimetallic Au@Ag Nanoparticles by Exploiting Eccentric Polymer Shells. *J. Am. Chem. Soc.* **2010**, *132*, 9537–9539.
28. Xing, S. X.; Tan, L. H.; Chen, T.; Yang, Y. H.; Chen, H. Y. Facile Fabrication of Triple-Layer (Au@Ag)@Polypyrrole Core−Shell and (Au@H_2O)@Polypyrrole Yolk−Shell Nanostructures. *Chem. Commun.* **2009**, *13*, 1653–1654.
29. Duesterberg, C. K.; Mylon, S. E.; Waite, T. D. pH Effects on Iron-Catalyzed Oxidation Using Fenton's Reagent. *Environ. Sci. Technol.* **2008**, *42*, 8522–8527.
30. Sun, Y. G.; Mayers, B.; Herricks, T.; Xia, Y. N. Polyol Synthesis of Uniform Silver Nanowires: A Plausible Growth Mechanism and the Supporting Evidence. *Nano Lett.* **2003**, *3*, 955–960.
31. Cho, E. C.; Cobley, C. M.; Rycenga, M.; Xia, Y. N. Fine Tuning the Optical Properties of Au−Ag Nanocages by Selectively Etching Ag with Oxygen and a Water-Soluble Thiol. *J. Mater. Chem.* **2009**, *19*, 6317–6320.
32. Zhang, Q.; Cobley, C. M.; Zeng, J.; Wen, L. P.; Chen, J. Y.; Xia, Y. N. Dissolving Ag from Au−Ag Alloy Nanoboxes with H_2O_2: A Method for Both Tailoring the Optical Properties and Measuring the H_2O_2 Concentration. *J. Phys. Chem. C* **2010**, *114*, 6396–6400.
33. Chen, H. Y.; Gao, Y.; Zhang, H. R.; Liu, L. B.; Yu, H. C.; Tian, H. F.; Xie, S. S.; Li, J. Q. Transmission-Electron-Microscopy Study on Fivefold Twinned Silver Nanorods. *J. Phys. Chem. B* **2004**, *108*, 12038–12043.
34. Gao, Y.; Gao, Y.; Song, L.; Jiang, P.; Liu, L. F.; Yan, X. Q.; Zhou, Z. P.; Liu, D. F.; Wang, J. X.; Yuan, H. J.; *et al.* Silver Nanowires with Five-Fold Symmetric Cross-Section. *J. Cryst. Growth* **2005**, *276*, 606–612.
35. Soukoulis, C. M.; Kafesaki, M.; Economou, E. N. Negative-Index Materials: New Frontiers in Optics. *Adv. Mater.* **2006**, *18*, 1941–1952.
36. Liu, N.; Giessen, H. Coupling Effects in Optical Metamaterials. *Angew. Chem., Int. Ed.* **2010**, *49*, 9838–9852.